Title

Engineering the Interface of Ceria and Silver Janus Nanoparticles for Enhanced Catalytic Performance in 4-Nitrophenol Conversion

Journal

ACS Applied Nano Materials, 6(10)

ISSN

2574-0970

Authors

Pallares, Roger M

Karstens, Sarah L

Arino, Trevor

et al.

Publication Date

2023-05-26

DOI

10.1021/acsanm.3c01394

ACS APPLIED NANO MATERIALS

www.acsanm.org

Letter

Engineering the Interface of Ceria and Silver Janus Nanoparticles for Enhanced Catalytic Performance in 4-Nitrophenol Conversion

Roger M. Pallares, Sarah L. Karstens, Trevor Arino, Andrew M. Minor, and Rebecca J. Abergel*

Cite This: *ACS Appl. Nano Mater.* 2023, 6, 8141−8145

Read Online

ACCESS | Metrics & More | Article Recommendations | Supporting Information

ABSTRACT: In this work, we present a modified simultaneous growth and self-aggregation method that produces ceria and silver Janus nanoparticles for the conversion of 4-nitrophenol, a chemical widely used in several industries. The nanoparticles had cerium-to-silver ratios ranging from 0 to 1.35 and well-defined heterodimer morphologies. By controlling the growth conditions, we have manipulated the interface between ceria and silver, maximizing its exposure to the chemical reactants and increasing the reaction rate constants between 2- and 4-fold. Taken together, these results can inform the design rules to achieve better performing hybrid nanocatalysts.

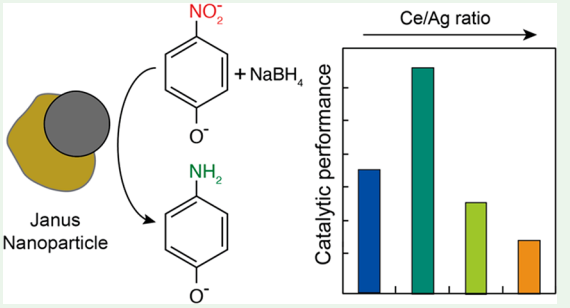

KEYWORDS: *nanocatalysts, Janus nanoparticles, hybrid nanoparticles, ceria, silver nanoparticles, catalysis*

Many industrial processes, from synthesis of pharmaceuticals to petroleum refining, require the use of catalysts.[1,2] In this context, metal nanocrystals offer unique opportunities, as they display strong catalytic performances and high surface-to-volume ratios, which can be enhanced by tailoring their size and shape.[3,4] While traditional nanocatalysts used to be made of single elements, such as silver or platinum, in recent years multicomponent nanoparticles have attracted a lot of attention, as they can present advanced multifunctionalities.[5,6] For example, silver and ceria nanocomposites take advantage of the strong catalytic activity of the former (due to its electronic cloud) and the rich redox behavior of the latter because of the oxygen vacancy defects generated when shifting between Ce(III) and Ce(IV) oxidation states. Hence, ceria and silver nanocomposites have been explored in heterogeneous catalytic reactions, including alcohol oxidation, soot oxidation and nitrophenol reduction,[7−9] and photocatalytic reactions.[10]

The synthesis of nanoparticles that simultaneously display noble metal and ceria parts is particularly challenging, as noble metals and ceria tend to grow separately because of their low affinity and strong immiscibility. Recent developments in wet colloidal synthesis have started to overcome those limitations through redox coprecipitation,[11] seed-mediated approaches,[12] and simultaneous growth and self-aggregation methods.[13,14] Nevertheless, when combining the two components in a single catalyst, it is important to preserve their individual features. For example, the reported catalytic performance of ceria and noble metal nanoparticles is widely variable in the literature, ranging from highly catalytic to poorly catalytic.[9,10,13,15,16] This variation is believed to be caused by the degree of interface exposure because (nano)ceria is not catalytic[13,16] and needs to be in close contact with the metal. For instance, if the ceria shell covers the noble metal core, the resulting nanocomposite shows poorer catalytic activity.[13] Hence, fine control over the nanoparticle structure is necessary to maximize the access of the reagents to the interface between ceria and silver and promote the reactions.

Here, we present a modified one-pot method to prepare hybrid ceria and silver nanocrystals with heterodimer structures via simultaneous growth and self-aggregation (Scheme 1). By controlling the growth conditions, we

Scheme 1. Synthesis and Catalytic Performance of Janus Nanoparticles

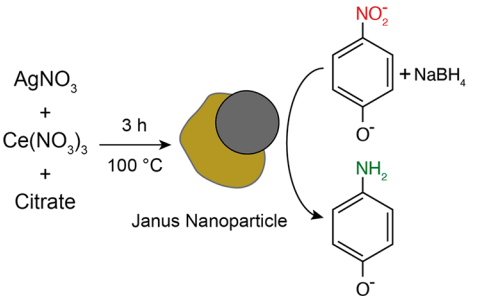

Received: March 29, 2023
Accepted: May 2, 2023
Published: May 8, 2023

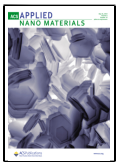

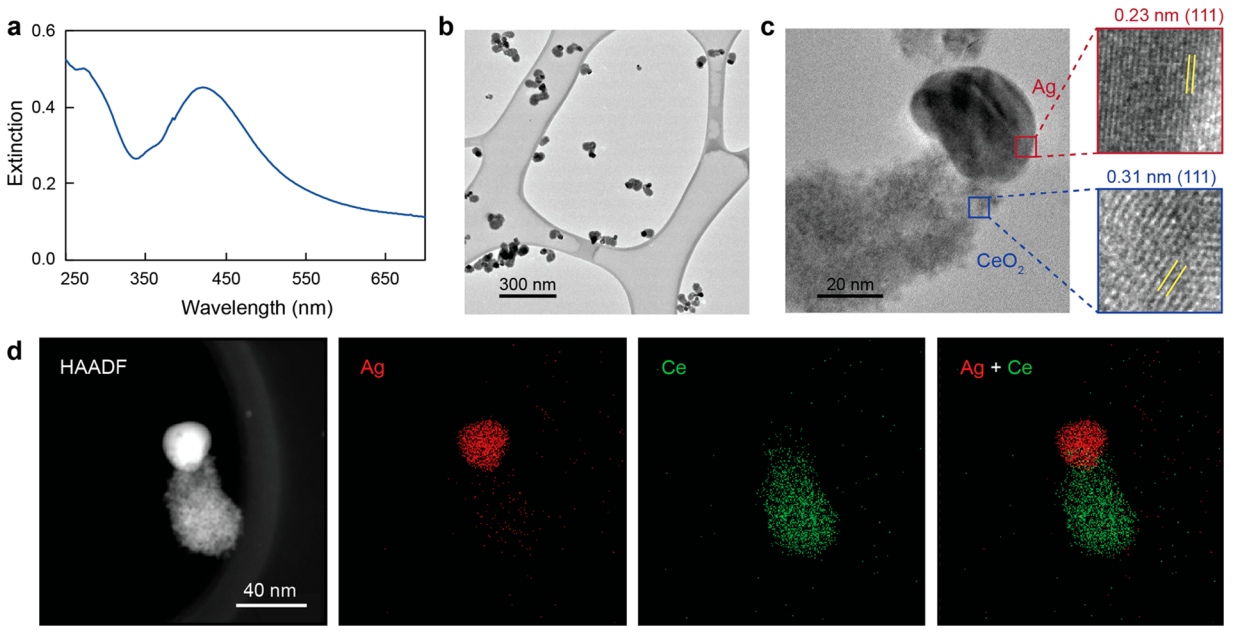

Figure 1. Characterization of Janus CeAg-1 nanoparticles. (a) UV−vis spectrum of nanoparticles in aqueous solution. (b) Bright field and (c) high-resolution transmission electron microscopy images of CeAg-1. The insets show the characteristic (111) crystal planes of ceria and silver. (d) High-angle annular dark-field electron micrograph and elemental mapping of representative CeAg-1 nanoparticle.

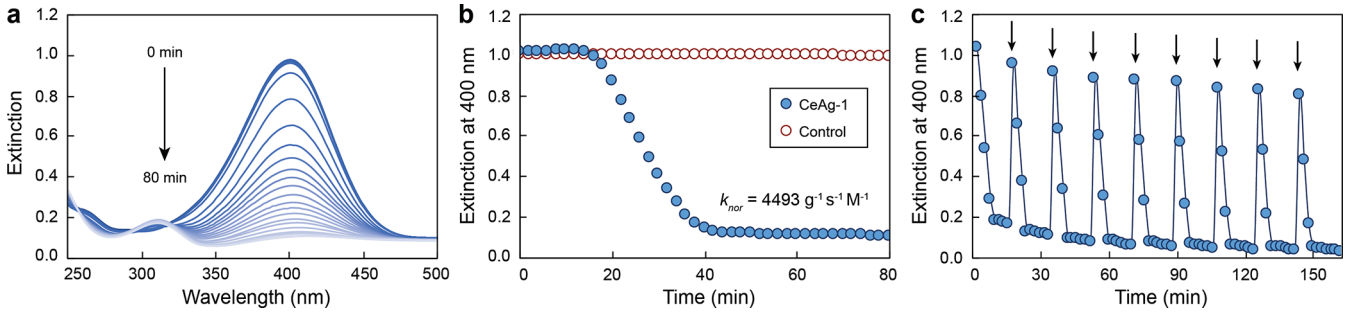

Figure 2. Catalytic performance of Janus CeAg-1 nanoparticles. (a) UV−vis spectrum of 4-nitrophenolate hydrogenation in the presence of CeAg-1 and 600-fold excess of sodium borohydride. (b) Catalytic kinetics of 4-nitrophenolate conversion in the presence and absence (control) of CeAg-1 (12 μg of CeAg-1). (c) Reuse of CeAg-1 in multiple catalytic cycles. In order to accelerate the catalytic reaction, the catalyst amount was increased (48 μg of CeAg-1). Arrows indicate time points when fresh 4-nitrophenol was added into the solution.

manipulated the morphology of the nanoparticles and engineered the interface between ceria and silver to maximize the conversion of 4-nitrophenol into 4-aminophenol. The latter is a chemical widely used in the production of pharmaceuticals, dyes, and lubricants, and its synthesis via 4-nitrophenol hydrogenation only occurs in the presence of catalysts.[17] We identified that there is an optimal ratio between silver and ceria, which maximizes interface exposure to the chemical reactants, yielding greater catalytic rate constants. Beyond this optimal point, larger amounts of ceria in the hybrid nanoparticles have a detrimental effect, as ceria starts covering the silver parts, quenching its catalytic effect.

Janus nanoparticles made of ceria and silver were synthesized via one-pot synthesis in aqueous media. Silver nitrate and cerium(III) nitrate were mixed in a solution of sodium citrate and refluxed for 3 h (for details refer to the Experimental Section in the Supporting Information). Citrate acts as both reducing and stabilizing agent of silver ions. Moreover, citrate molecules complex cerium(III) ions, which undergo oxidation and hydrolysis before depositing on the silver nanoparticles.[14] The resulting solutions had a brown-yellow color, and their UV−vis spectra (Figure 1a) displayed bands centered at 278 and 422 nm, which are characteristic of ceria and silver nanoparticles, respectively.[18−20] The Janus nanoparticles (CeAg-1) had heterodimer structures made of silver and ceria components with ferret diameters of 18 ± 4 and 35 ± 6 nm, respectively (Figure 1b). In addition, the molar ratio between Ce and Ag was 0.95 (Table S1), as determined by nanoparticle acidic digestion and mass spectrometry (following a previous published protocol[21−23]).

Interestingly, ceria did not form shells on top of silver nanoparticles, likely due to the large lattice mismatch between silver and ceria (lattice parameters of 4.09 and 5.41 Å, respectively[24,25]), which favored the formation of heterodimer nanoparticles rather than core−shell ones. Nevertheless, despite the lattice mismatch, the majority of nanoparticles in the sample (94%) were formed by both ceria and silver components, as observed by electron microscopy. High-resolution transmission electron microscopy demonstrated the crystal structure of CeAg-1, where characteristic (111) planes of both silver and ceria were observed (Figure 1c). Moreover, the elemental composition and heterodimer

https://doi.org/10.1021/acsanm.3c01394
ACS Appl. Nano Mater. 2023, 6, 8141−8145

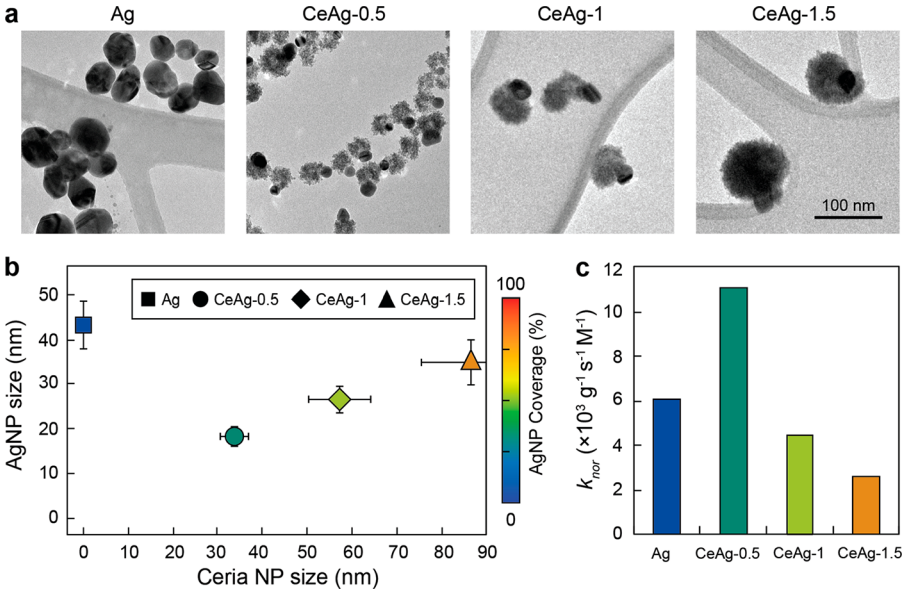

Figure 3. Effect of nanoparticle morphology on catalytic performance. (a) Transmission electron micrographs of selected nanoparticles. All micrographs are displayed at the same scale. (b) Size of silver and ceria nanoparticles (AgNP and Ceria NP, respectively) and fraction of silver covered by ceria. (c) Normalized rate constants (k_{nor}) for each nanoparticle.

structure of CeAg-1 were further confirmed by elemental mapping via energy-dispersive X-ray spectroscopy (Figures 1d and S1).

The catalytic performance of CeAg-1 was evaluated by measuring the conversion of 4-nitrophenol to 4-aminophenol by sodium borohydride in water. The reaction can be easily monitored under basic conditions by UV−vis spectroscopy because 4-nitrophenolate (anionic form of 4-nitrophenol) displays a characteristic band centered at 400 nm that disappears when the reagent is hydrogenated. The addition of CeAg-1 into a solution containing 4-nitrophenolate and sodium borohydride caused a gradual decrease (increase) of the band at 400 nm (310 nm), indicating the catalytic reduction of 4-nitrophenolate (Figure 2a). However, in the absence of CeAg-1 (control), the reaction did not progress (Figure 2b). The 600-fold excess of sodium borohydride with respect to 4-nitrophenolate allowed to consider the catalytic conversion as pseudo-first-order reaction (Figure S2). Thus, we calculated a normalized rate constant (k_{nor}) for CeAg-1 of 4493 g^{-1} s^{-1} M^{-1}, which is greater than the k_{nor} of other common nanocatalysts, including platinum, palladium, and gold nanoparticles (Table S2).[26,27] The kinetic data also showed an induction time of 16 min. Induction times in the order of minutes had been commonly reported in the literature for other nanocatalysts.[28−30] Although this phenomenon is still not fully understood, it seems to be defined by multiple factors, including the concentration of catalyst and reagents in solution,[31,32] the adsorption rate of reagent on the nanoparticle surface,[33] and reagent-induced restructuring of the nanoparticle surface.[34,35]

Next, we confirmed that CeAg-1 could be reused in multiple consecutive catalytic cycles (Figure 2c). 4-Nitrophenol was repeatedly added into a solution that contained the nanoparticles and a large excess of sodium borohydride and sodium hydroxide. The new 4-nitrophenol was spiked in the solution after the reagent from the previous cycle had been totally consumed. This process was performed in nine occasions resulting in complete 4-nitrophenol consumption.

As previously described, the catalytic performance of ceria and noble metal nanoparticles is widely variable in the literature,[9,10,13,15,16] as it has been hypothesized that ceria may be beneficial or detrimental depending on its content and its distribution on nanoparticles. Hence, we decided to explore the role of ceria on the performance of our heterodimer nanocatalyst by synthesizing four nanoparticle samples with different proportions of $Ce(NO_3)_3$ and $AgNO_3$. After the washing step, the elemental compositions of the nanoparticles were characterized by mass spectrometry (Table S1). The four nanoparticle types (Figure 3a) had Ce to Ag molar ratios of 0.00, 0.51, 0.95, and 1.34 and were labeled as Ag, CeAg-0.5, CeAg-1, and CeAg-1.5, respectively. Except for the Ag sample, increasing the ratio of cerium(III), increased the size of both silver and ceria particles (Figure 3b). While it is reasonable that larger amounts of cerium(III) yield bigger ceria nanoparticles, their connection to the size of silver nanoparticles is less clear. We hypothesize that the cerium fluid oxidation state, which easily switches between +3 and +4, might have affected the reduction of silver ions and the final nanoparticle sizes.

It is worth noting that increasing the cerium/silver ratio not only affected the size of ceria and silver particulates, but also other nanoparticle characteristics, including their spatial distribution (Figure 3b). As the cerium/silver ratio increased, so did the fraction of silver nanoparticle covered by ceria, which ranged from 0 (Ag) to 72% (CeAg-1.5). To identify the impact of silver exposure on the catalytic performance of the Janus nanoparticles, we characterized 4-nitrophenolate conversion in the presence of the different nanocolloids. Although all Janus nanoparticles promoted the hydrogenation of 4-nitrophenolate (Figures S2 and S3), they showed rather different catalytic performances (Figure 3c). On the one hand, CeAg-0.5 was the best performing nanocatalyst because it displayed the largest k_{nor}. It contained both silver and ceria components, and a large fraction of the silver particulate (65.5 ± 23.8%) was exposed to the medium (not covered by ceria), allowing its interaction with the reagent. Moreover, CeAg-0.5 also displayed smaller silver particulates, which are likely to be

https://doi.org/10.1021/acsanm.3c01394
ACS Appl. Nano Mater. 2023, 6, 8141−8145

more efficient because of their higher surface-to-mass ratio. On the other hand, CeAg-1 and CeAg-1.5 showed smaller k_{nor} than Ag (bare silver nanoparticles). It is worth noting that silver nanoparticles are the active components of the nanocatalysts, and ceria only enhances the performance of silver at their interface. Ceria by itself has no catalytic activity.[13,16] Taking the above into consideration, we hypothesize that when ceria covers the majority of the silver nanoparticle surface, it hampers the interaction between 4-nitrophenolate and silver, preventing the catalytic reaction. This observation is consistent with previous studies exploring the use of ceria and other noble metals.[13]

In summary, we have exploited a modified one-pot method to produce hybrid nanoparticles made of ceria and silver via simultaneous growth and self-aggregation. By controlling the growth conditions, we were able to manipulate the interface between ceria and silver, and to identify their effects in the catalytic conversion of 4-nitrophenol. Our study highlights the ceria-to-silver ratio of 0.53 as optimal for catalytic performance because larger ceria content decreased the exposure of silver to the reactant-rich environment, decreasing the catalytic reaction rate constants. Hence, our study demonstrates that not only the components of nanocatalysts are important but also their spatial distribution and 3D structure. Taken together, we expect that this work will provide new design rules and opportunities in the engineering of nanoparticle-based catalysts.

■ ASSOCIATED CONTENT

Supporting Information

The Supporting Information is available free of charge at https://pubs.acs.org/doi/10.1021/acsanm.3c01394.

Experimental section, quantification of Ce and Ag content in nanoparticles by mass spectrometry, energy-dispersive X-ray spectrum of CeAg-1, linearized kinetic data for first-order analysis, comparison of catalytic performance, UV−vis spectra of 4-nitrophenol hydrogenation in the presence of nanoparticles (PDF)

■ AUTHOR INFORMATION

Corresponding Author

Rebecca J. Abergel − *Chemical Sciences Division, Lawrence Berkeley National Laboratory, Berkeley, California 94720, United States; Department of Nuclear Engineering, University of California, Berkeley, Berkeley, California 94720, United States;* orcid.org/0000-0002-3906-8761; Email: abergel@berkeley.edu

Authors

Roger M. Pallares − *Chemical Sciences Division, Lawrence Berkeley National Laboratory, Berkeley, California 94720, United States; Institute for Experimental Molecular Imaging (ExMI), RWTH Aachen University Hospital, Aachen 52074, Germany;* orcid.org/0000-0001-7423-8706

Sarah L. Karstens − *National Center for Electron Microscopy, Molecular Foundry, Lawrence Berkeley National Laboratory, Berkeley, California 94720, United States; Department of Chemistry, University of California, Berkeley, Berkeley, California 94720, United States*

Trevor Arino − *Chemical Sciences Division, Lawrence Berkeley National Laboratory, Berkeley, California 94720, United States; Department of Nuclear Engineering, University of California, Berkeley, Berkeley, California 94720, United States*

Andrew M. Minor − *National Center for Electron Microscopy, Molecular Foundry, Lawrence Berkeley National Laboratory, Berkeley, California 94720, United States; Department of Materials Science and Engineering, University of California, Berkeley, Berkeley, California 94720, United States*

Complete contact information is available at: https://pubs.acs.org/10.1021/acsanm.3c01394

Notes

The authors declare no competing financial interest.

■ ACKNOWLEDGMENTS

This work was supported by the U.S. Department of Energy (DOE), Office of Science, Office of Basic Energy Sciences, Chemical Sciences, Geosciences, and Biosciences Division, Heavy Element Chemistry Program (RJA) and Materials Sciences and Engineering Division, Electron Microscopy of Soft Matter Program (AMM), at the Lawrence Berkeley National Laboratory under Contract DE-AC02-05CH11231. Work at the Molecular Foundry was supported by the Office of Science, Office of Basic Energy Sciences, of the U.S. DOE under Contract DE-AC02-05CH11231.

■ REFERENCES

(1) Busacca, C. A.; Fandrick, D. R.; Song, J. J.; Senanayake, C. H. The Growing Impact of Catalysis in the Pharmaceutical Industry. *Adv. Synth. Catal.* **2011**, *353* (11−12), 1825−1864.

(2) Environmental Catalysis: Mobile Sources. In *Fundamentals of Industrial Catalytic Processes*; 2005; pp 705−752.

(3) Astruc, D. Introduction: Nanoparticles in Catalysis. *Chem. Rev.* **2020**, *120* (2), 461−463.

(4) Xie, C.; Niu, Z.; Kim, D.; Li, M.; Yang, P. Surface and Interface Control in Nanoparticle Catalysis. *Chem. Rev.* **2020**, *120* (2), 1184−1249.

(5) Wu, Z.; Li, L.; Liao, T.; Chen, X.; Jiang, W.; Luo, W.; Yang, J.; Sun, Z. Janus nanoarchitectures: From structural design to catalytic applications. *Nano Today* **2018**, *22*, 62−82.

(6) Pallares, R. M.; Abergel, R. J. Transforming lanthanide and actinide chemistry with nanoparticles. *Nanoscale* **2020**, *12* (3), 1339−1348.

(7) Beier, M. J.; Hansen, T. W.; Grunwaldt, J.-D. Selective liquid-phase oxidation of alcohols catalyzed by a silver-based catalyst promoted by the presence of ceria. *J. Catal.* **2009**, *266* (2), 320−330.

(8) Shimizu, K.-i.; Kawachi, H.; Satsuma, A. Study of active sites and mechanism for soot oxidation by silver-loaded ceria catalyst. *Appl. Catal. B: Environmental* **2010**, *96* (1), 169−175.

(9) Chernykh, M.; Mikheeva, N.; Zaikovskii, V.; Salaev, M.; Liotta, L. F.; Mamontov, G. Room-Temperature Nitrophenol Reduction over Ag−CeO_2 Catalysts: The Role of Catalyst Preparation Method. *Catalysts* **2020**, *10*, 580.

(10) Zhao, S.; Riedel, M.; Patarroyo, J.; Bastús, N. G.; Puntes, V.; Yue, Z.; Lisdat, F.; Parak, W. J. Tailoring of the photocatalytic activity of CeO_2 nanoparticles by the presence of plasmonic Ag nanoparticles. *Nanoscale* **2022**, *14* (33), 12048−12059.

(11) Mitsudome, T.; Yamamoto, M.; Maeno, Z.; Mizugaki, T.; Jitsukawa, K.; Kaneda, K. One-step Synthesis of Core-Gold/Shell-Ceria Nanomaterial and Its Catalysis for Highly Selective Semihydrogenation of Alkynes. *J. Am. Chem. Soc.* **2015**, *137* (42), 13452−13455.

(12) Piella, J.; Gónzalez-Febles, A.; Patarroyo, J.; Arbiol, J.; Bastús, N. G.; Puntes, V. Seeded-Growth Aqueous Synthesis of Colloidal-Stable Citrate-Stabilized Au/CeO_2 Hybrid Nanocrystals: Heterodimers, Core@Shell, and Clover- and Star-Like Structures. *Chem. Mater.* **2019**, *31* (19), 7922−7932.

(13) Bastús, N. G.; Piella, J.; Perez, S.; Patarroyo, J.; Genç, A.; Arbiol, J.; Puntes, V. Robust one-pot synthesis of citrate-stabilized Au@CeO_2 hybrid nanocrystals with different thickness and dimensionality. *Appl. Mater. Today* **2019**, *15*, 445−452.
(14) Patarroyo, J.; Delgado, J. A.; Merkoçi, F.; Genç, A.; Sauthier, G.; Llorca, J.; Arbiol, J.; Bastus, N. G.; Godard, C.; Claver, C.; Puntes, V. Hollow PdAg-CeO_2 heterodimer nanocrystals as highly structured heterogeneous catalysts. *Sci. Rep.* **2019**, *9* (1), 18776.
(15) Yi, N.; Si, R.; Saltsburg, H.; Flytzani-Stephanopoulos, M. Steam reforming of methanol over ceria and gold-ceria nanoshapes. *Appl. Catal. B: Environmental* **2010**, *95* (1), 87−92.
(16) Liu, B.; Yu, S.; Wang, Q.; Hu, W.; Jing, P.; Liu, Y.; Jia, W.; Liu, Y.; Liu, L.; Zhang, J. Hollow mesoporous ceria nanoreactors with enhanced activity and stability for catalytic application. *Chem. Commun.* **2013**, *49* (36), 3757−3759.
(17) Kong, X.; Zhu, H.; Chen, C.; Huang, G.; Chen, Q. Insights into the reduction of 4-nitrophenol to 4-aminophenol on catalysts. *Chem. Phys. Lett.* **2017**, *684*, 148−152.
(18) Calvache-Muñoz, J.; Prado, F. A.; Rodríguez-Páez, J. E. Cerium oxide nanoparticles: Synthesis, characterization and tentative mechanism of particle formation. *Colloids Surf., A* **2017**, *529*, 146−159.
(19) Choi, B.-h.; Lee, H.-H.; Jin, S.; Chun, S.; Kim, S.-H. Characterization of the optical properties of silver nanoparticle films. *Nanotechnology* **2007**, *18* (7), 075706.
(20) Singh, S.; Bharti, A.; Meena, V. K. Green synthesis of multi-shaped silver nanoparticles: optical, morphological and antibacterial properties. *J. Mater. Sci.: Mater. Electron.* **2015**, *26* (6), 3638−3648.
(21) Yue, J.; Pallares, R. M.; Cole, L. E.; Coughlin, E. E.; Mirkin, C. A.; Lee, A.; Odom, T. W. Smaller CpG-Conjugated Gold Nanoconstructs Achieve Higher Targeting Specificity of Immune Activation. *ACS Appl. Mater. Interfaces* **2018**, *10* (26), 21920−21926.
(22) Pallares, R. M.; Choo, P.; Cole, L. E.; Mirkin, C. A.; Lee, A.; Odom, T. W. Manipulating Immune Activation of Macrophages by Tuning the Oligonucleotide Composition of Gold Nanoparticles. *Bioconjugate Chem.* **2019**, *30* (7), 2032−2037.
(23) Pallares, R. M.; Carter, K. P.; Zeltmann, S. E.; Tratnjek, T.; Minor, A. M.; Abergel, R. J. Selective Lanthanide Sensing with Gold Nanoparticles and Hydroxypyridinone Chelators. *Inorg. Chem.* **2020**, *59* (3), 2030−2036.
(24) Fan, Z.; Zhang, H. Template Synthesis of Noble Metal Nanocrystals with Unusual Crystal Structures and Their Catalytic Applications. *Acc. Chem. Res.* **2016**, *49* (12), 2841−2850.
(25) Stojmenović, M.; Žunić, M.; Gulicovski, J.; Bajuk-Bogdanović, D.; Holclajtner-Antunović, I.; Dodevski, V.; Mentus, S. Structural, morphological, and electrical properties of doped ceria as a solid electrolyte for intermediate-temperature solid oxide fuel cells. *J. Mater. Sci.* **2015**, *50* (10), 3781−3794.
(26) Mourdikoudis, S.; Altantzis, T.; Liz-Marzán, L. M.; Bals, S.; Pastoriza-Santos, I.; Pérez-Juste, J. Hydrophilic Pt nanoflowers: synthesis, crystallographic analysis and catalytic performance. *CrystEngComm* **2016**, *18* (19), 3422−3427.
(27) Mourdikoudis, S.; Montes-García, V.; Rodal-Cedeira, S.; Winckelmans, N.; Pérez-Juste, I.; Wu, H.; Bals, S.; Pérez-Juste, J.; Pastoriza-Santos, I. Highly porous palladium nanodendrites: wet-chemical synthesis, electron tomography and catalytic activity. *Dalton Trans.* **2019**, *48* (11), 3758−3767.
(28) Nigra, M. M.; Ha, J.-M.; Katz, A. Identification of site requirements for reduction of 4-nitrophenol using gold nanoparticle catalysts. *Catalysis Science & Technology* **2013**, *3* (11), 2976−2983.
(29) Satapathy, S. S.; Bhol, P.; Chakkarambath, A.; Mohanta, J.; Samantaray, K.; Bhat, S. K.; Panda, S. K.; Mohanty, P. S.; Si, S. Thermo-responsive PNIPAM-metal hybrids: An efficient nanocatalyst for the reduction of 4-nitrophenol. *Appl. Surf. Sci.* **2017**, *420*, 753−763.
(30) Gao, S.; Zhang, Z.; Liu, K.; Dong, B. Direct evidence of plasmonic enhancement on catalytic reduction of 4-nitrophenol over silver nanoparticles supported on flexible fibrous networks. *Appl. Catal. B: Environmental* **2016**, *188*, 245−252.
(31) Neal, R. D.; Inoue, Y.; Hughes, R. A.; Neretina, S. Catalytic Reduction of 4-Nitrophenol by Gold Catalysts: The Influence of Borohydride Concentration on the Induction Time. *J. Phys. Chem. C* **2019**, *123* (20), 12894−12901.
(32) Chakraborty, S.; Ansar, S. M.; Stroud, J. G.; Kitchens, C. L. Comparison of Colloidal versus Supported Gold Nanoparticle Catalysis. *J. Phys. Chem. C* **2018**, *122* (14), 7749−7758.
(33) Zeng, J.; Zhang, Q.; Chen, J.; Xia, Y. A Comparison Study of the Catalytic Properties of Au-Based Nanocages, Nanoboxes, and Nanoparticles. *Nano Lett.* **2010**, *10* (1), 30−35.
(34) Wunder, S.; Polzer, F.; Lu, Y.; Mei, Y.; Ballauff, M. Kinetic Analysis of Catalytic Reduction of 4-Nitrophenol by Metallic Nanoparticles Immobilized in Spherical Polyelectrolyte Brushes. *J. Phys. Chem. C* **2010**, *114* (19), 8814−8820.
(35) Wunder, S.; Lu, Y.; Albrecht, M.; Ballauff, M. Catalytic Activity of Faceted Gold Nanoparticles Studied by a Model Reaction: Evidence for Substrate-Induced Surface Restructuring. *ACS Catal.* **2011**, *1* (8), 908−916.

https://doi.org/10.1021/acsanm.3c01394
ACS Appl. Nano Mater. 2023, 6, 8141−8145